Measurement of Radio-Frequency Magnetic Fluctuations in the VTF Magnetic Reconnection Experiment

by

JOHN PETER WHITNEY

Submitted to the Department of Physics
in partial fulfillment of the requirements for the degree of

BACHELOR OF SCIENCE

at the

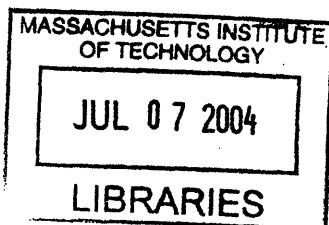MASSACHUSETTS INSTITUTE OF TECHNOLOGY

May 2004 [June 2004]

Author . . . .
Department of Physics
May 7, 2004

Certified by . . . .
Miklos Porkolab
Professor of Physics
Thesis Supervisor

Accepted by . . . .
David E. Pritchard
Senior Thesis Coordinator, Department of Physics

Measurement of Radio-Frequency Magnetic Fluctuations in the VTF Magnetic Reconnection Experiment

by

John Peter Whitney

Abstract

In this thesis work, I designed, fabricated, and calibrated, a radio-frequency magnetic probe, subsequently used to measure magnetic turbulance in the reconnecting plasmas of the Versatile Toroidal Facility (VTF). Reconnecting Hydrogen plasmas were created, and magnetic fluctuations in all three cartesian directions were measured in the 1-100MHz range. A preliminary hodogram analysis of the fluctuation spectra found the propagation direction of low-frequency (1-5MHz) electromagnetic waves to be parallel to the direction of the plasma current, while high-frequency waves had a random distribution of propagation directions.

Acknowledgments

I would like to recognize and thank the many people, that without their help, this thesis would have never been successful. I would like to thank Will Fox, for his infinite supply of help in electronics, Physics, and understanding of the practical considerations and theoretical basis for the experiment. I am indebted to Jan Egedal, who first brought me onto the project, came up with invaluable solutions to many problems, and provided an almost magical ability to "make it work". The largest and most appreciated contributions from both Will and Jan were the uncounted hours they spent assisting my work, and their consistent patience with me. I must also thank Dave Cylinder, Hantao Ji, Stephen Terry, and Masaaki Yamada for their excellent guidance, which prepared me for work on this thesis project. I am also greatful to Steve Wukitch, who provided a wonderful design concept for the probe, and to the entire RF division of the PSFC, for putting up with my constant "theft" of their equipment. Professor Porkolab, my advisor, deserves great thanks for his assistance in securing funding, providing administrative clout, and guiding the direction and scope of this research.

Contents

List of Figures

Chapter 1

Introduction to Magnetic Reconnection

1.1 The Phenomenon of Magnetic Reconnection

Magnetic reconnection is a physical process describing changes in magnetic field topology in plasmas. Specifically, magnetic reconnection concerns the breaking and rejoining of field lines, which is accompanied by a transfer of magnetic field energy into kinetic energy. Magnetic reconnection has been attributed to several instabilities in tokomak fusion devices [1]. These instabilities, such as the sawtooth instability, lead to anomalous particle and heat transport, and loss of plasma confinement. Magnetic reconnection has also been observed in the Earth's magnetosphere, where plasma from the solar wind interacts with the Earth's magnetic fields, leading in one instance to the Aurora phenomenon [1]. Magnetic reconnection is also thought to be the driving process in solar flares and other astrophysical processes involving plasma-magnetic field interactions.

Figure 1-1 shows a typical arrangement of field lines in a reconnection process. In this instance, the plasma is pulled apart in the horizontal direction, while drawing plasma in from the top and bottom, in a process called "pull reconnection". The reverse process, equally valid, is called "push reconnection". In the situation depicted in Figure 1-1, the incoming plasma is attached to the bunching field lines. As
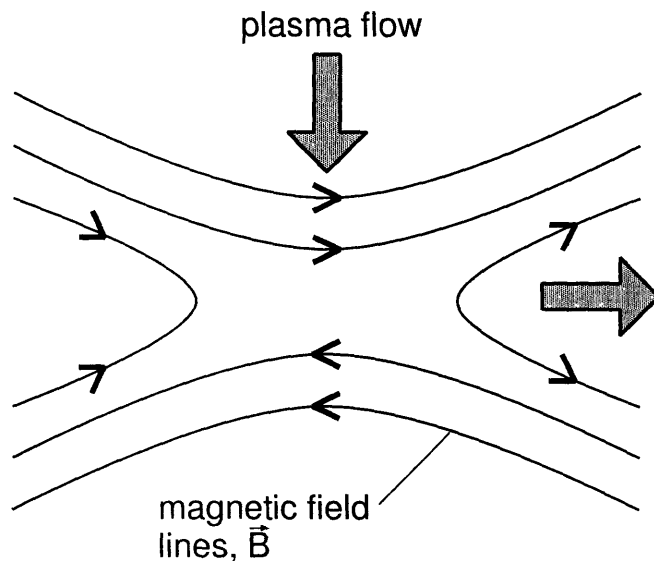
11

plasma flow

magnetic field
lines, $\vec{B}$

Figure 1-1: Typical reconnection magnetic field configuration.

the oppositely directed field lines continue to press together, they eventually break, and reform as the field lines shown with the ">" and "<" shapes. The field lines transition from a high-energy state, where the oppositely directed field lines are very close together, to a lower energy state, where they are separated from each other. This relaxation process transfers the extra magnetic energy to kinetic energy of the outflowing plasma.

1.2   Sweet-Parker Model of Reconnection

To gain a better physical understanding of the magnetic reconnection process, a good starting place is the simplest and original MHD[1] model of reconnection: the Sweet-Parker model. Figure 1-2 shows the basic geometry. For conducting plasmas, as the oppositely directed field lines are pressed together, an out-of-plane current is generated, forming a long, thin line of current, called a current sheet.

In the Sweet-Parker model, we assume steady-state conditions, with constant inflow and outflow velocities, $\vec{u}$ and $\vec{v}$, respectively, and we assume the fluid is incompressible. The thickness and length of the current sheet are δ and L. We write down

---

[1]MHD stands for Magnetohydrodynamics, in which plasmas are modeled as magnetized fluids.
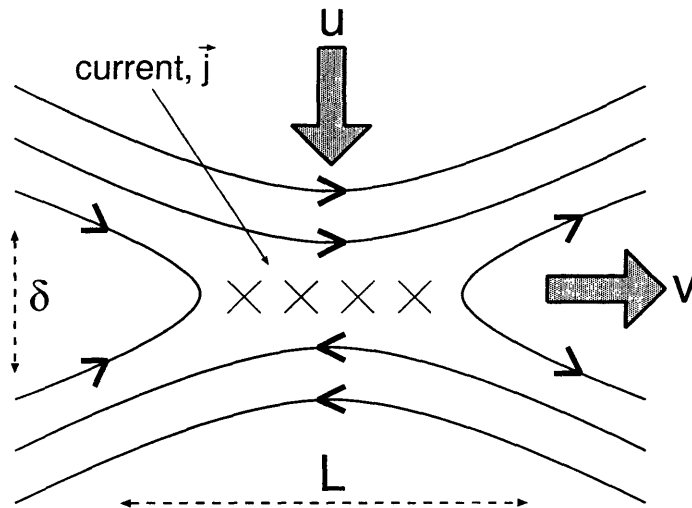
Figure 1-2: Sweet-Parker current sheet model.

the steady-state momentum equation[2]:

$$\rho(\vec{v} \cdot \vec{\nabla})\vec{v} = -\vec{\nabla}\left(p + \frac{B^2}{8\pi}\right),$$ (1.1)

Faraday's Law:

$$\frac{\partial \vec{B}}{\partial t} = \vec{\nabla} \times (\vec{v} \times \vec{B}),$$ (1.2)

and Ohm's Law,

$$\vec{E} + \frac{\vec{v} \times \vec{B}}{c} = \eta\vec{j},$$ (1.3)

where ρ is the plasma density, p is the pressure, and η is the resistivity of the plasma.

When the momentum equation is integrated along linear inflow and outflow directions, and combined with Faraday's and Ohm's Law, we find the characteristic reconnection time[3],

$$\tau_{rec} = \sqrt{\tau_A \tau_R}.$$ (1.4)

---

[2] All equations are in CGS units.

[3] The details of this derivation have been omitted, and are found in several introductary treatments of magnetic reconnection [1].

The Alfvén time, $\tau_A = L\sqrt{4\pi\rho}/B$, is the fastest time a field line can move in when the plasma is a perfect conductor. The time in which a field line can diffuse, when the plasma is resistive, is given by $\tau_R = 4\pi L^2 \eta c^2$. All timescales are relative to the linear scale of the region, which in this model is the current sheet length, L. In resistive plasmas, τ_R can be many times larger than τ_A. The essense of this model is that the formation of a current sheet develops a resistive zone, allowing for faster reconnection. The reconnection time is decreased from τ_R to $\sqrt{\tau_R \tau_A}$. This model seems to describe things nicely, but unfortunately it fails to accurately predict the real reconnection rates for many physical plasmas. In the case of a solar flare, the reconnection time is measured on the order of minutes, while the Sweet-Parker model predicts a reconnection time on the order of months. The bulk of reconnection research is aimed at explaining why the reconnection rate is so high, by trying to understand what additional physics must be included.

1.3 Fast Reconnection Theories

Most fast reconnection theories introduce additional physics through Ohm's Law. The complete form of Ohm's Law is written [3]

$$\underbrace{\vec{E} + \frac{\vec{v} \times \vec{B}}{c}}_{resistive\ MHD} = \eta\vec{j} + \underbrace{\eta^*\vec{j}}_{anom.\ \eta} + \underbrace{\frac{\vec{j} \times \vec{B}}{nec}}_{Hall} + \frac{\vec{\nabla} \cdot \vec{P}}{ne} + \underbrace{\frac{m_e}{e^2}\vec{V_e} \cdot \nabla\frac{\vec{j}}{n}}_{inertia}, \tag{1.5}$$

where n is the number density, η^* is the anomalous plasma resistivity, e is the electron charge, and m_e is the electron mass.

Currently, researchers are concentrating on the Hall term and the anomalous resistivity term. The two effects are somewhat mutually exclusive, as the Hall situation uses laminar flows, while the anomalous resistivity is based on turbulance in the current sheet. While the theoretical investigations of these two phenomena are quite numerous (though far from conclusive), there has been very limited experimental observation of either effect. Additionally, other researchers believe the important physics lie either in the off-diagonal terms of the pressure tensor, or in the physics of

14

electron orbits.

This thesis work begins an experimental investigation of the role of turbulance in fast reconnection. The basic idea in turbulance theories is that electromagnetic turbulance scatters electrons in the plasma, leading to an increase in the plasma resistivity. In an idealized perfectly conducting plasma, the electrons are able to instantaneously rearrange themselves in order to negate any movement of the magnetic fields, according to Lenz's Law. In this case, the field lines can only move if the plasma moves, thus leading to a description of the field lines as "frozen in". As the resistance of the plasma increases, the field lines can move faster, relative to the plasma rest frame. If there is electromagnetic turbulance, then scattering events can prevent electrons from rearranging as quickly, leading to higher plasma resistivity and faster reconnection.

In order for this effect to matter, there must be some source of free energy to feed the fluctuations. In the Sweet-Parker picture of reconnection, this free energy is found in the density and pressure gradients across the current sheet. Besides providing a mechanism for fluctuations to occur, the current sheet also provides a boundary to trap them. The situation is analagous to the Quantum Mechanics picture of particles trapped in a potential well. Just as in the quantum analogy, these fluctuations can form spatially localized modes. Figure 1-3 shows an example of this situation. In this figure, the horizontal axis corresponds to the vertical axes of Figures 1-1 and 1-2, taking a slice through the null-point. The figure shows sample current and fluctuation profiles inside the current sheet, although the fluctuation amplitude is shown exaggerated. Trying to predict the fluctuation modes theoretically has been the subject of recent research [2]. That research seems to indicate that the magnetic fluctuations should be peaked in the center of the current sheet, with dominant even-order modes.

The type of fluctuations that are generated is hotly debated, and unresolved [3]. Just a few of the instabilities considered are the Lower Hybrid Drift Instability (LHDI), Modified Two-Stream Instability (MTSI), and the Drift Kink Instability (DKI) [3]. These are just a few. Recent interest has focused on LHDI, and related instabilities. The experiments carried out in this work are designed to cast as wide
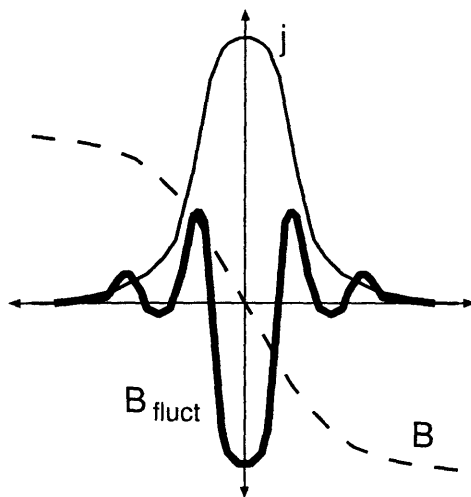
Figure 1-3: Example of a trapped magnetic mode in plasma current sheet.

a net as possible, trying to measure fluctuations over as large a range of wavelengths and frequencies as is experimentally possible.

Of particular concern is the frequency range in which we expect the fluctuations to be. LHDI and MTSI fluctuations both have a distribution of frequencies on the order of $\sqrt{f_i f_e}$. If electrons in VTF have a gyro-frequency of $2.45GHz$, then Hydrogen has an ion gyrofrequency of $2.45GHz/1836$, leading to a LHDI frequency of $2.45GHz/\sqrt{1836} \approx 57MHz$. For Argon, this reduces to $9MHz$. These fluctuations may have a broad frequency spectra, a topic which is discussed in detail in the literature [3]. The goal of the present experiment is only to make a survey of the excited frequencies. Essentially, we are interested in exploring the frequency range between the ion and electron gyro-frequencies, which in the VTF experiment lies in the radio-frequency domain.

Chapter 2

VTF Experiment

2.1 Overview

The Versitile Toroidal Facility (VTF) is a large toroidal plasma chamber with a rectangular cross-section, located in the Plasma Science Fusion Center (PSFC) at The Massachusetts Institute of Technology (MIT) [4]. Plasmas are generated by electron cyclotron resonance heating (ECRH), using a 2.45GHz microwave beam. Figure 2.1 shows a cross section of the vacuum vessel. The experiment also has a series of toroidal field (TF) coils, used to generate a guide field in the theta (out of page) direction. Figure 2-1 shows the experiment in what is called the open-field configuration, where the field lines do not connect into loops inside the walls of the chamber. Figure 2-2 shows schematically the field behavior when operating in the open configuration.

The VTF experiment has recently been modified to operate in a closed-field configuration. To achieve this, there are two sets of internal single-loop coils, shown as the four circles in Figure 2-3. The inner poloidal field (PF) solenoid coils, shown in Figure 2-1, are connected to a capacitor bank, and constitute the so-called slow drive. When the cap-bank is discharged, a current is induced in the same direction through all four loops, creating the familiar quadrupolar magnetic field configuration discussed in Chapter 1. Then, another cap-bank discharges, which is wired so that the top and bottom pairs of loops carry current in opposite directions. This so-called
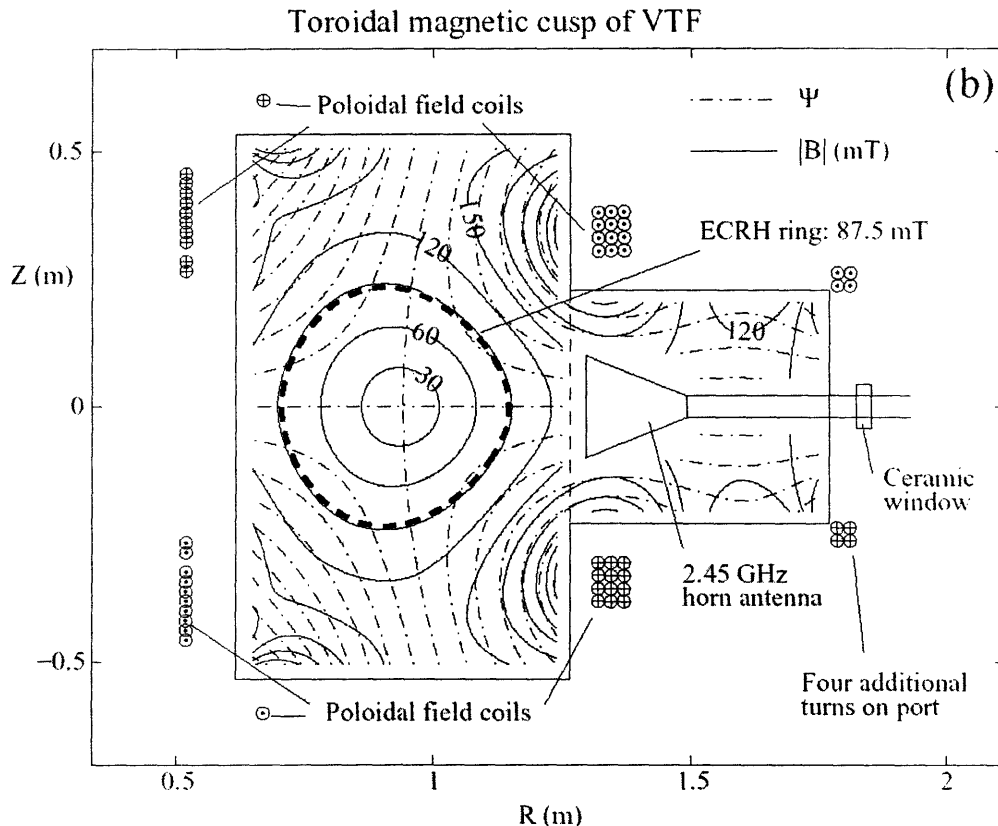
Toroidal magnetic cusp of VTF

Figure 2-1: VTF vacuum vessel cross-section (open configuration).

fast drive is used to alternately push and pull flux through the null point, driving fast magnetic reconnection. Figure 2-3 shows the field behavior due to the fast drive. The fast drive completes several reconnection cycles before it is completely discharged. The closed configuration coils were installed and wired in late March 2004. They are also positioned conviniently to allow operation in the open configuration, without interfering with the plasma.

Figure 2-4 shows a comparison of the important parameters of several reconnection experiments.[1] One of the most unique and significant advantages that the VTF machine has over other reconnection experiments is its ability to operate in very colli-

---

[1]Symbols defined: L is the length scale, n_e is the electron number density, T_e is the electron temperature, T_i is the ion temperature, B is the nominal field strength, m_i/m_p is the ion to proton mass ratio, ρ_i/L is the normalized ion gyroradius, c/ω_{pi} is the ion skin depth, c/ω_{ei} is the electron skin depth, λ_e is the mean free path, and S is the Lundquist number, $S = \tau_R/\tau_A$.
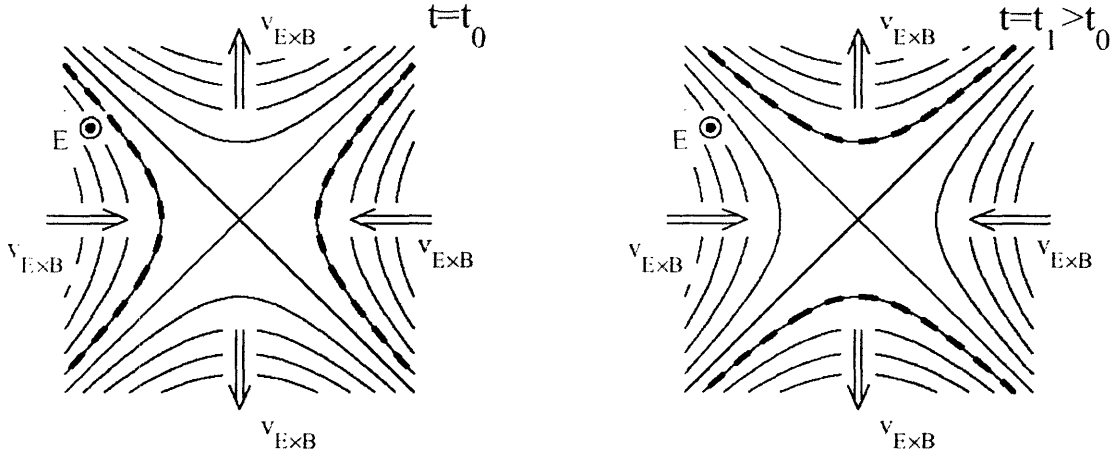
18

Figure 2-2: Reconnection x-line geometry in VTF open configuration.

sionless regimes, seen in Figure 2-4 in a comparison of collisional mean free path to an experiments length scale. VTF, unlike some other experiments, can run with many different gases. The microwave heating method is also beneficial because ohmic heating methods used on other experiments link, rather than separate, the reconnection and plasma formation processes.

VTF has a suite of diagnostics, used to measure many properties of the plasma during an experiment. There is a 20-channel magnetic probe array, with the pick-up coils mounted on a horizontal arm that can be raised and lowered. There is also a similarly mounted 45-channel Langmuir probe array, used to measure the plasma temperature and density profiles. Mach probes are used to measure the 3D plasma flows. A gridded energy analyser is used to measure the parallel velocity distribution of ions. We have yet to apply the full battery of diagnostics to the closed configuration, as it has only recently been installed.
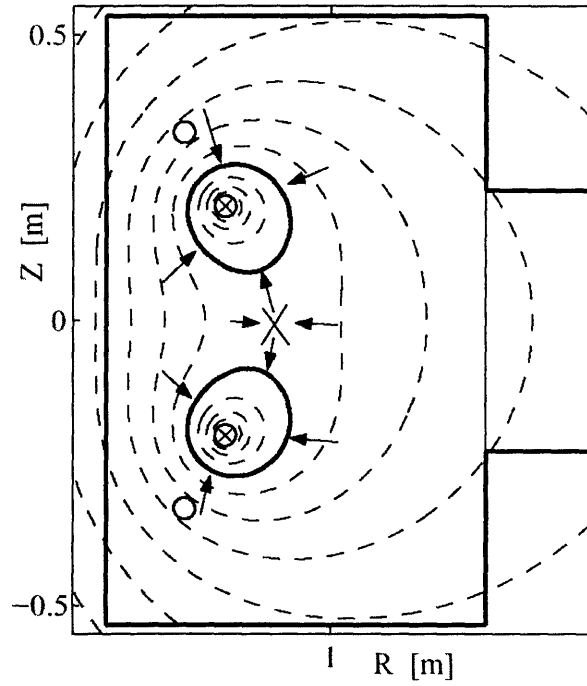
Figure 2-3: VTF closed configuration coils and subsequent fields.

Parameter	MRX	LCD	TS-D3	VTF open	VTF closed
L [m]	0.1	0.3	0.1	0.5	0.2
n_e [m^{-3}]	$10^{19} - 10^{20}$	10^{18}	$5 \cdot 10^{20}$	$2 \cdot 10^{17}$	$10^{17} - 10^{19}$
T_e [eV]	20	10	10	20	5 — 60
T_i [eV]	10	2	10	2	2 — 15
B [T]	0.05	$2 \cdot 10^{-3}$	0.5	0.03 – 0.09	0.03 – 0.09
m_i/m_p	1	40	4	1 — 40	1 — 40
ρ_i/L	0.08	2	0.01	0.03 – 0.09	0.02 — 0.6
c/ω_{pi} [m]	0.02	0.6	$2 \cdot 10^{-3}$	0.5 — 3	0.07 — 5
c/ω_{pe} [m]	$5 \cdot 10^{-4}$	$5 \cdot 10^{-3}$	$2 \cdot 10^{-4}$	0.01	0.002 – 0.02
λ_e [m]	0.002 – 0.1	1	$1 \cdot 10^{-3}$	10 — 100	0.1 — 10^3
S	900	60	700	900	150 — 4500

Figure 2-4: Parameter comparison between several reconnection experiments.

Chapter 3

FastB Probe

3.1 Design and Calibration

To measure magnetic fluctuations, we will use small magnetic induction coils. Imagine
a situation depicted in Figure 3-1. An electromagnetic wave travels in the vertical
direction, and has a wavelength larger than the coil diameter. If the polarization is as
shown, there will be some dB/dt component in the horizontal direction. A changing
magnetic flux induces a voltage across the coil according to

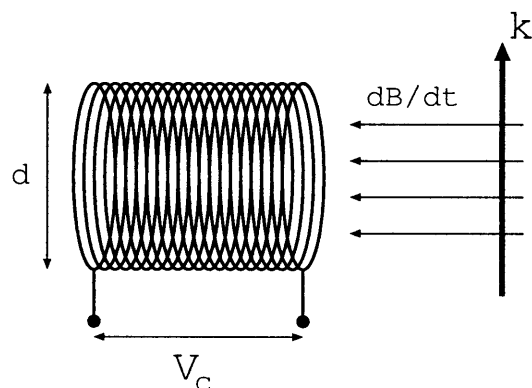$$V_c = NA\frac{dB}{dt},\tag{3.1}$$

Figure 3-1: FastB coil.

where N is the number of turns in the coil, and A is the cross-sectional area of the

coil. For a sinusoidally varying magnetic field we can rewrite this equation as,

$$V_c = NAB\omega, \tag{3.2}$$

where V_c, and B are the peak amplitudes of sinusoidally varying signals with frequency, ω. The result here is that the signal measured increases linearly with frequency. However, this can not increase forever; as the frequency rises, the impedance of the coil due to its self-inductance also rises linearly. In Figure 3-2, we show both the probe and calibration setup circuit models, including the inductance and resistance associated with the probe. The coil internal resistance will be small enough to be neglected. Solving for the probe voltage, V_p, as a function of the fluctuation induced voltage, V_c, we obtain

$$V_p = \frac{50NAB\omega}{\sqrt{50^2 + (\omega L_c)^2}}. \tag{3.3}$$

Thus, when $\omega L_c \gg 50$, the probe voltage is reduced to $50NAB/L_c$, or a constant, independent of frequency. The termination is 50Ω because at radio frequencies, impedance matching of the transmission line is necessary to prevent reflected signals and radiation losses. To calibrate the probe, a test field is generated with a Helmholtz coil. This arrangement consists of two identical circular coils spaced by a distance equal to the coils' radius. This common method generates a very uniform field in the central region between the coils. The calibration setup is shown in Figure 3-2. An HP 8656B signal generator was used to drive the Helmholtz coil at approximately 1 Volt. Critical to the calibration is the current measurement, which was done with a Pearson model 2877 current transformer. Using a current transformer avoids impedance matching issues when calibrating over a large frequency range.

There are also impedance matching issues on the probe end. Since the probe must handle a large range of frequencies, a surface-mount 50Ω resistor jumpered the leads of each coil. This divides the signal in two, but prevents mismatch problems at high frequencies. The coils were wound on $1mm$ diameter ceramic tubes, using 4 mil, enamel coated magnet wire. Each of the three coils had around 60 turns
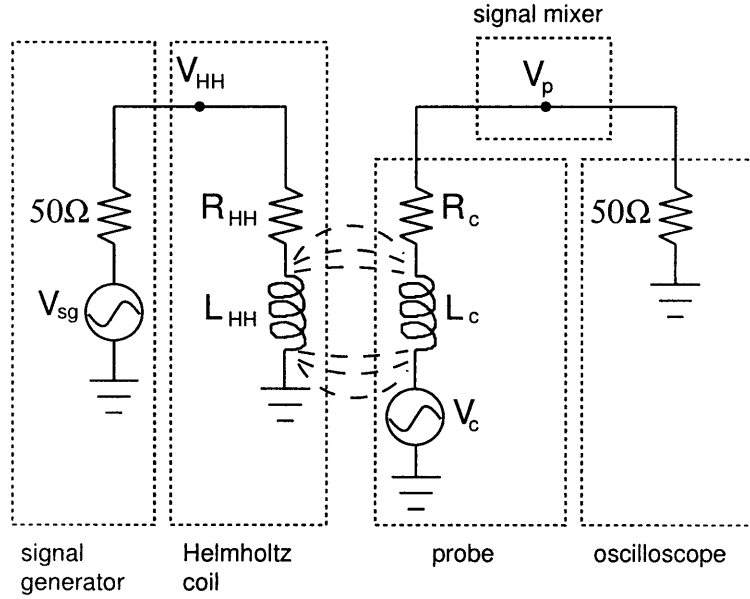
22

Figure 3-2: Circuit model for probe and calibration setup.

in four winding layers. Keeping the diameter as small as possible is necessary to allow sensitivity to as short a wavelength as possible; the coils are only sensitive to wavelengths longer than their diameter[1].

Three coils were arranged in a Cartesian configuration, and epoxied together. UT-85 microcoax was used to connect each lead (6 total, 2 per coil) from the coils. These then travel down the stainless steel probe shaft to RF signal mixers, Mini-Circuits model ZMSCJ-2-1. These are necessary to subtract out any electrostatic noise in the signal. These mixers are 50Ω matched, an have an operational bandwidth from $1 - 200MHz$. The signal then travels into a Tektronics TDS 5104 digitizing oscilloscope, terminated at 50Ω. This oscilloscope can digitize at up to $1.25GHz$.

The last $30cm$ of the business end of the probe is enclosed by a $9mm$ O.D. glass tube. The tube is attached to the stainless probe shaft through a vacuum-tight compression fitting. The probe shaft is attached to a metal bellows setup, which allows the probe to be moved radially through the vacuum chamber without breaking

---

[1]Predicting the fluctuation wavelengths is theoretically challenging. The MRX experiment, at the Princeton Plasma Physics Laboratory (PPPL), has made preliminary measurements under similar plasma conditions that show wavelengths on the order of 5cm, but we need to be prepared for possible shorter wavelengths.

vacuum. The positioning is controlled by a Unislide-brand, stepper motor-controlled, linear stage. The stepper motor is controlled by a VXM motor controller, which is attached to the oscilloscope computer via serial port. Both the oscilloscope and probe drive can be controlled by LabVIEW software in the control room over the LAN. Although not yet motorized, a custom flange was machined to allow the probe to tilt up and down inside the chamber, thus allowing off-axis fluctuation measurements.

After the probe was completed, but before its installation into the VTF machine, a calibration set was taken for all three coils. The results are shown in Figure 3-3. The probe coils were designed so that their response would be flat over the region of interest, and would give as large a signal as possible, while maintaining a minimum coil diameter. The coil parameters were set after completing a theoretical trade-off study, and a series of experimental investigations with different coil configurations.

The completed probe, just before installation, is shown in Figure 3-4 sitting on a workbench.
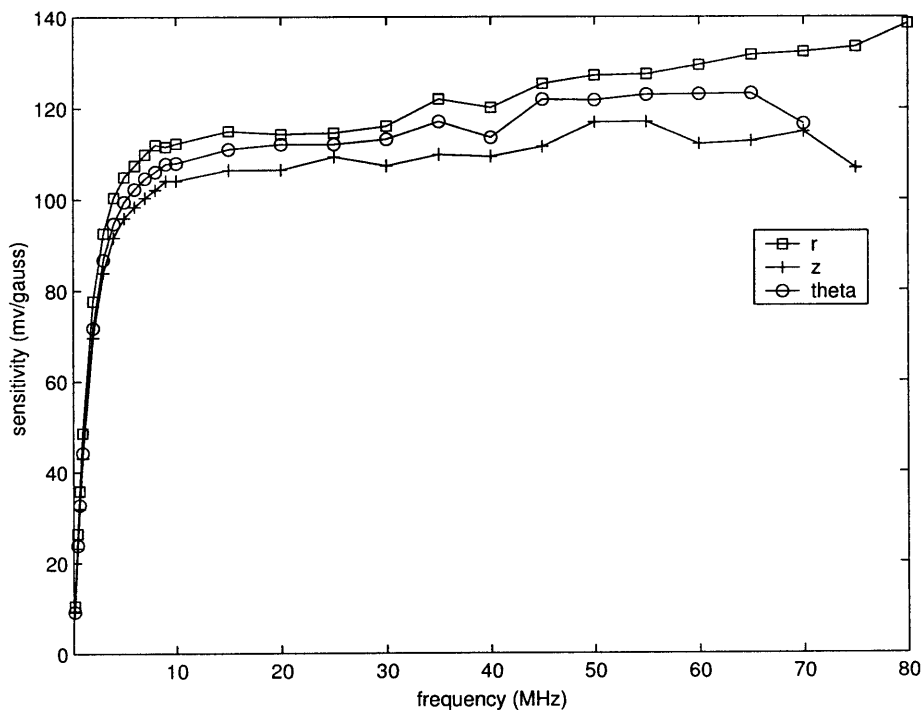

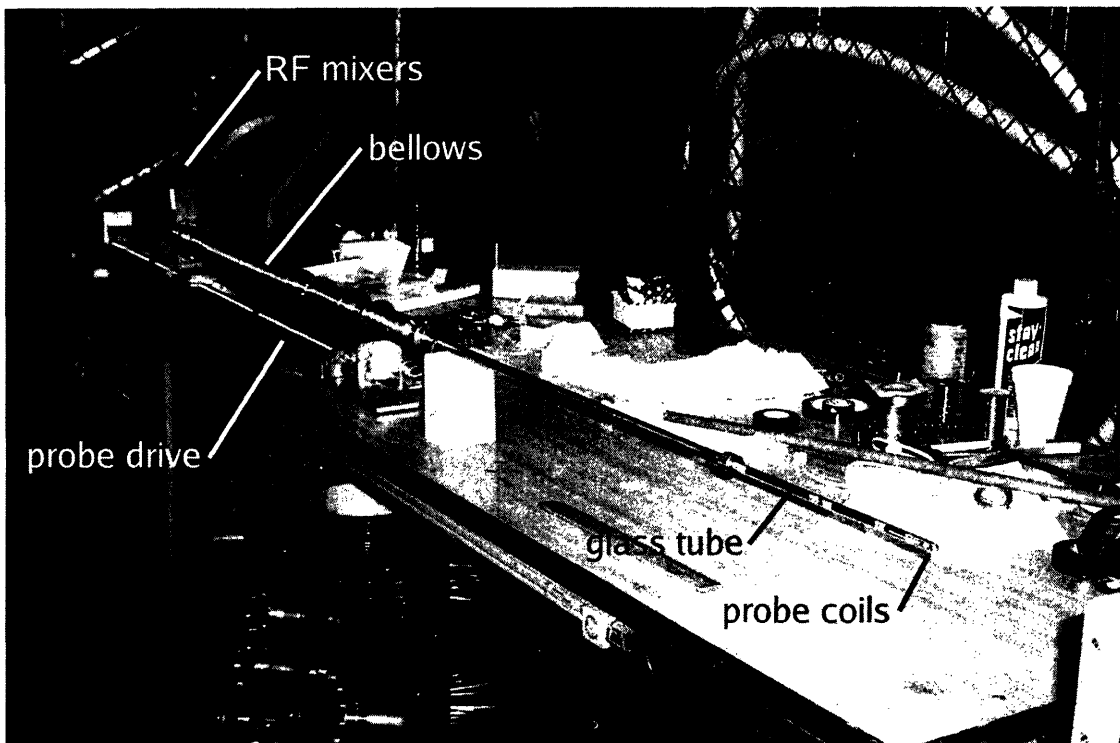Figure 3-3: Probe sensitivity over radio-frequency range.

24

Figure 3-4: FastB probe on workbench.

Chapter 4

Experimental Results

4.1   Overview of Measurements

After the installation of the closed configuration coils in late March 2004, the next few weeks were spent testing out the new system. It became clear that there was a learning curve to climb, in order to understand what voltages the fast and slow capacitor bank drives should be set to. For example, if the fast drive voltage was set too high relative to the slow drive, the plasma would be ripped into separate blobs, and a coherent current sheet would not develop. During this trial and error period, fluctuation data was collected with the FastB probe to test its performance and behavior. During this period where the closed configuration was still being tested, a high-voltage switch that connects the experiment to a high-voltage power grid line failed. Unfortunately, it will not be repaired until mid-May, after the completion of this thesis. Six weeks of time was lost, which was to be used to make extensive measurements with the FastB probe and other diagnostics, to fully characterize the plasma. The following presents the preliminary results obtained during the trial and error period.

4.2 Collected Data

Figure 4-1 shows data from one of the earliest shots taken, using Hydrogen gas. Here, the probe is located near the approximate center of the current sheet. The three fluctuation packets correspond to three cycles of the fast reconnection drive. The data was recorded in 500,000 samples, which over $2ms$ yields a sample rate of $250MHz$. Thus, we can resolve fluctuations up to the Nyquist frequency of $125MHz$. Figure 4-2 shows an enlargement of the first reconnection event, and its corresponding spectrogram. While the FFT in Figure 4-3 shows that the fluctuations are predominately below $10MHz$[1], there are higher frequency fluctuations at certain times during the reconnection event. It does seem, in this preliminary case, that fluctuations in the lower-hybrid range $(\approx 60MHz)$[2] are much lower amplitude than fluctuations in the ion gyro-frequency $(\approx 1MHz)$ range. This result has been observed in the MRX reconnection experiment [3], but is contradicted by later results on the same experiment [5]. Clearly it is premature to draw any conclusions from our results until after plasmas in the new configuration have been fully characterized and investigated.

Figure 4-4 shows the results of a sequence of 31 shots, moving the probe radially through the null-point. Each position, spaced by $1cm$ each, has a strip spectrogram[3] applied. The radial position is measured out from the center of the inner set of internal drive coils. We see that the lower frequency fluctuations appear first, followed by the high-frequency ones. Subsequently, the current sheet dissolves, as seen in the fourth frame.

Isolating the data from the $r = 11cm$ point, Figure 4-5 shows that position's spectrogram. The choppiness of the fluctuations is due to movement of the current sheet. A further study using several diagnostics will be used to fully measure and characterize the current sheet, and will then be compared to the fluctuations.

---

[1]The data shown had a $200kHz$ 6th order high-pass Butterworth filter applied, to remove small ground-loop signals and fluctuations associated with plasma flow.

[2]Recall from Chapter 1 that f_{LH} is estimated from the electron gyro-frequency, and thus represents only an approximation. Calculating the exact frequency spectra is a topic of current research [2].

[3]The spectrogram scale has been adjusted to accentuate the high-frequency portion of the spectrum.

$V_{slow} = 1.7\text{kV}$

$V_{fast} = 1.6\text{kV}$

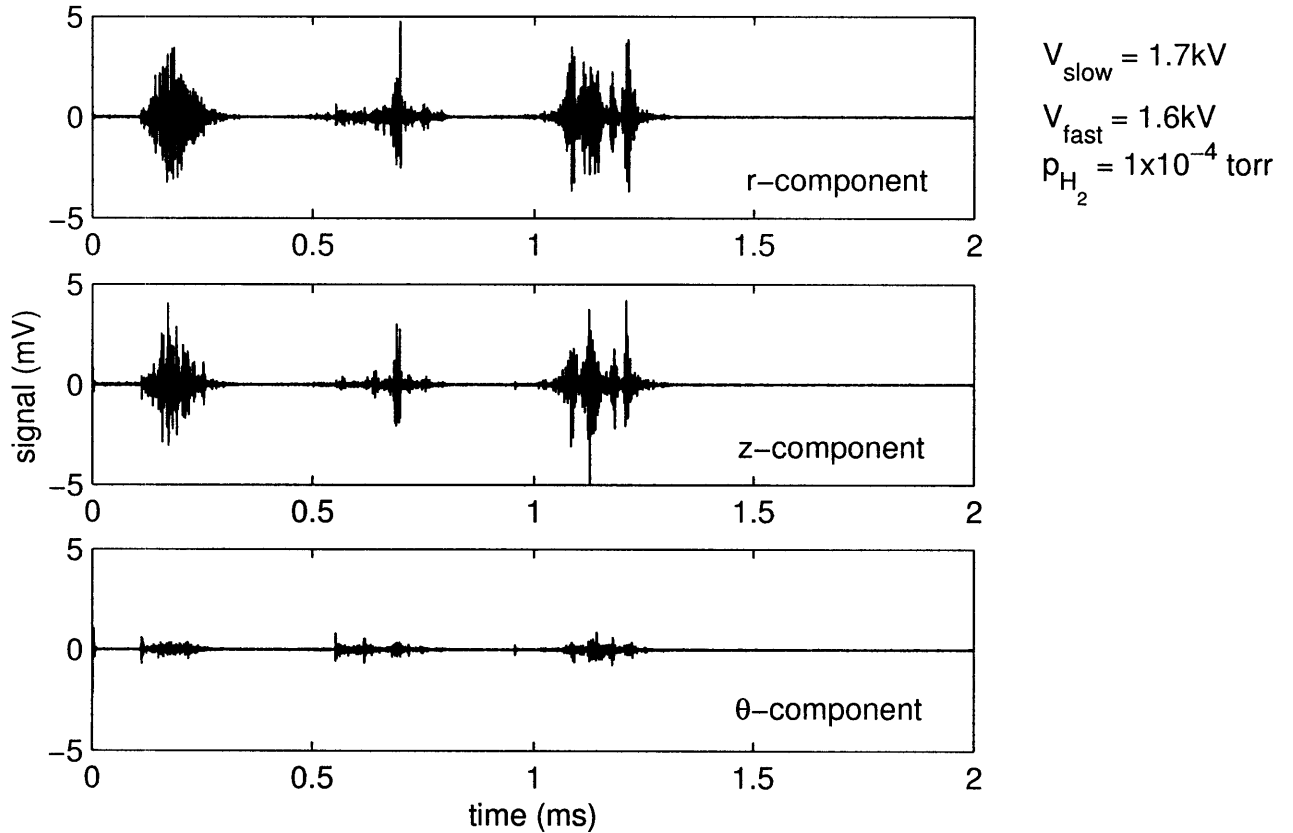$p_{H_2} = 1\text{x}10^{-4}\text{ torr}$

Figure 4-1: Sample AC-coupled signal from probe.

4.3 Hodogram Analysis

With this probe, even though we can only measure the components of the magnetic fluctuations, a technique called hodogram analysis can be used to measure the propagation direction of the electromagnetic fluctuations. The method makes use of the relation[4] $\vec{k} \cdot \vec{B} = 0$. Consider the magnetic field at two different times, t_0 and t_1, as shown in Figure 4-6. These two vectors form a plane, and $\vec{k}$ is perpendicular to them. Thus, the vector obtained by taking the cross-product, $\vec{B}(t_0) \times \vec{B}(t_1)$, is parallel to $\vec{k}$. We cannot find the magnitude of $\vec{k}$, but we can find its direction[5].

---

[4]Note that by using this condition we restrict ourself to examining only transverse waves.

[5]We actually know a little less than that; there is an overall sign ambiguity due to the sinusoidal nature of the waves measured, so we know the line parallel to $\vec{k}$, but we do not know the sign of $\vec{k}$
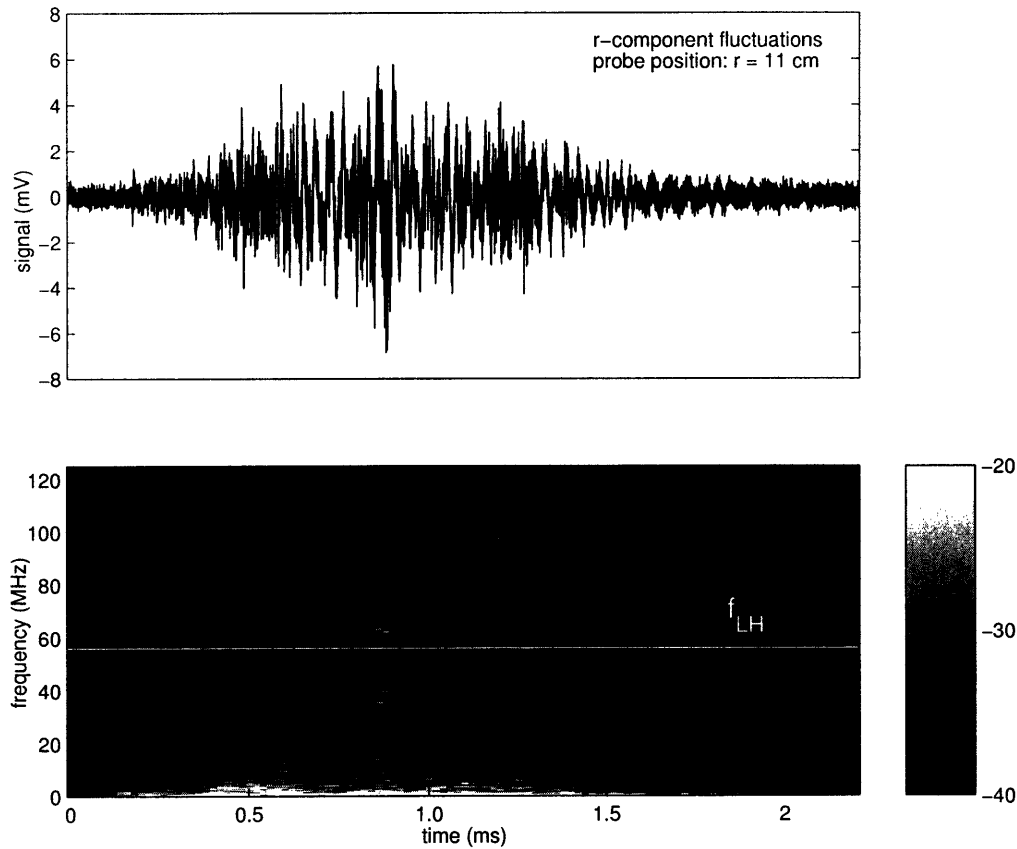
Figure 4-2: First reconnection event with matching spectrogram.

Figures 4-7 and 4-8 show the hodogram method applied to two different ranges of frequencies, and display the parallel (θ-direction) and perpendicular (in r-z plane) components of $\vec{k}$. Figure 4-9 shows the coordinate system for VTF; during reconnection, current is driven in the θ-direction. For low frequencies, shown in Figure 4-7, it is clear that waves travel in the θ-direction with only a very small perpendicular component. This makes sense given the relative magnitudes of the signals shown in Figure 4-1[6]. However, at high frequencies, there seem to be a mix of waves. The signal strength at these higher frequencies is probably too weak to provide accurate hodogram data.

These results are fairly consistent with recent results from the Princeton MRX

---

[6]Remember that a small θ-component means the waves are mostly travelling in that direction.
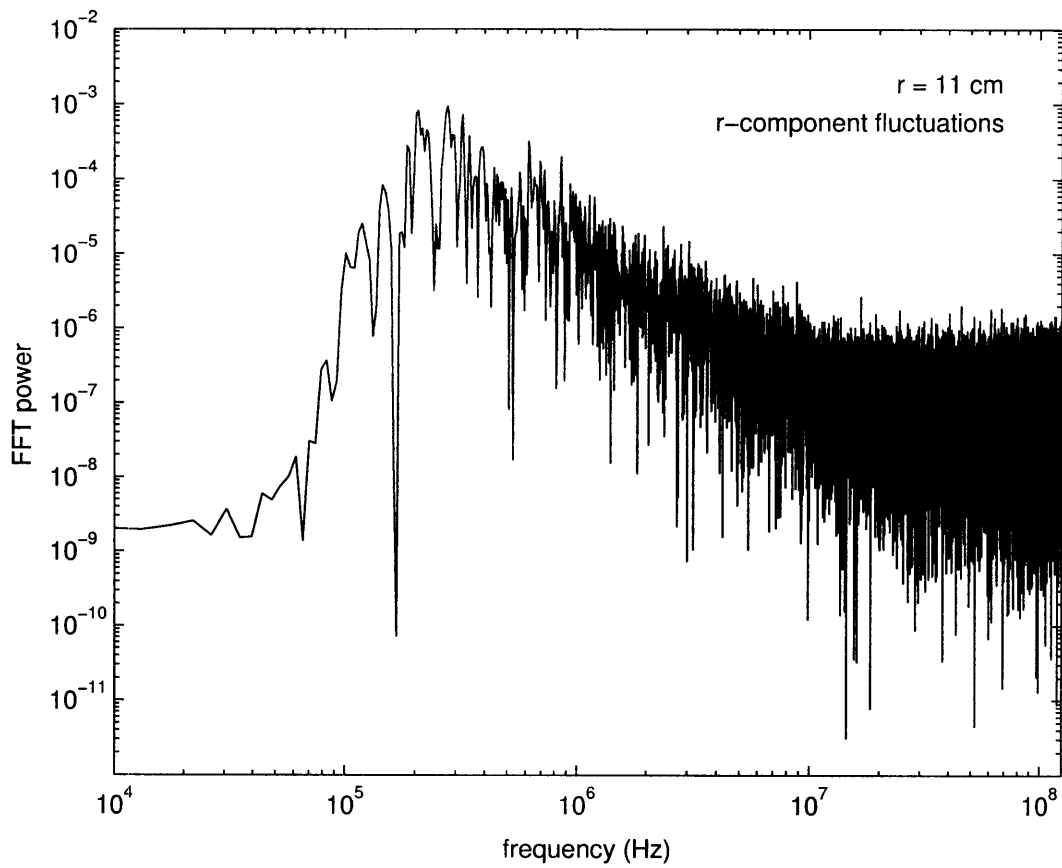
Figure 4-3: FFT plot for first reconnection event.

experiment [5], which showed low-frequency waves travelling in the θ-direction, and higher frequency waves more likely to travel at larger angles to the θ-direction.
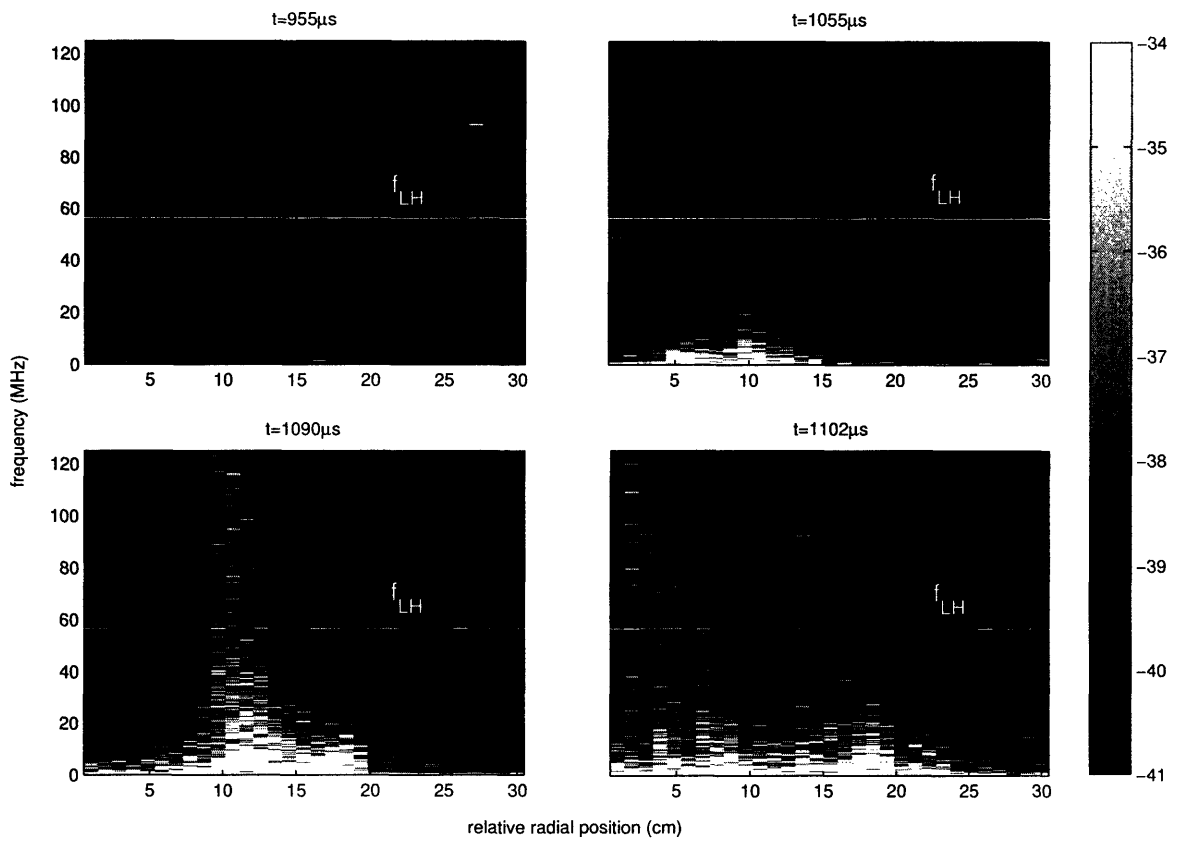
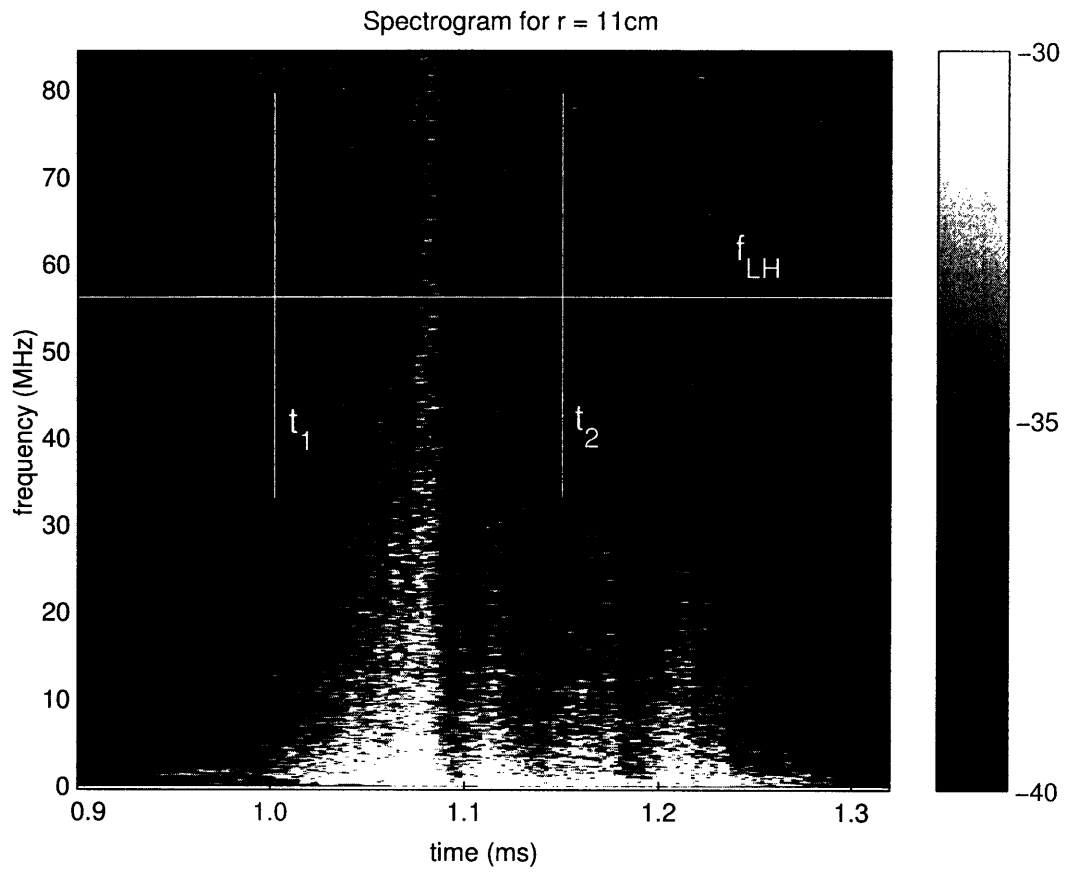Figure 4-4: Time-evolution of the radial fluctuation profile.
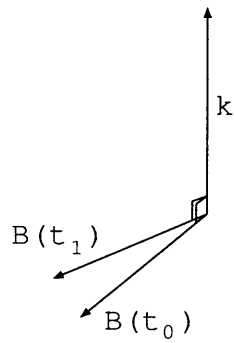
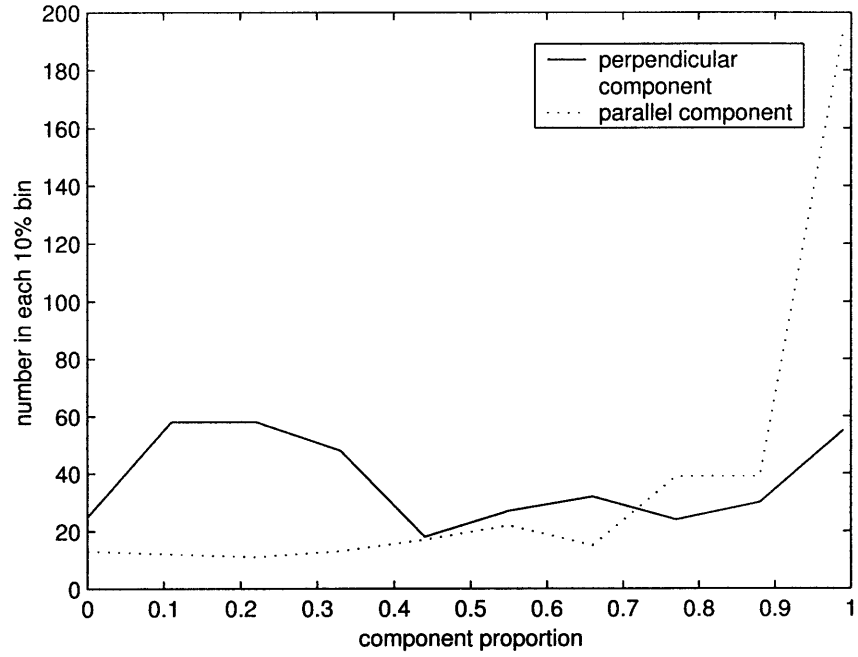Figure 4-5: Spectrogram of sample reconnection event.

Figure 4-6: Hodogram method

Figure 4-7: Hodogram plot for $f_{fluc} < 5MHz$

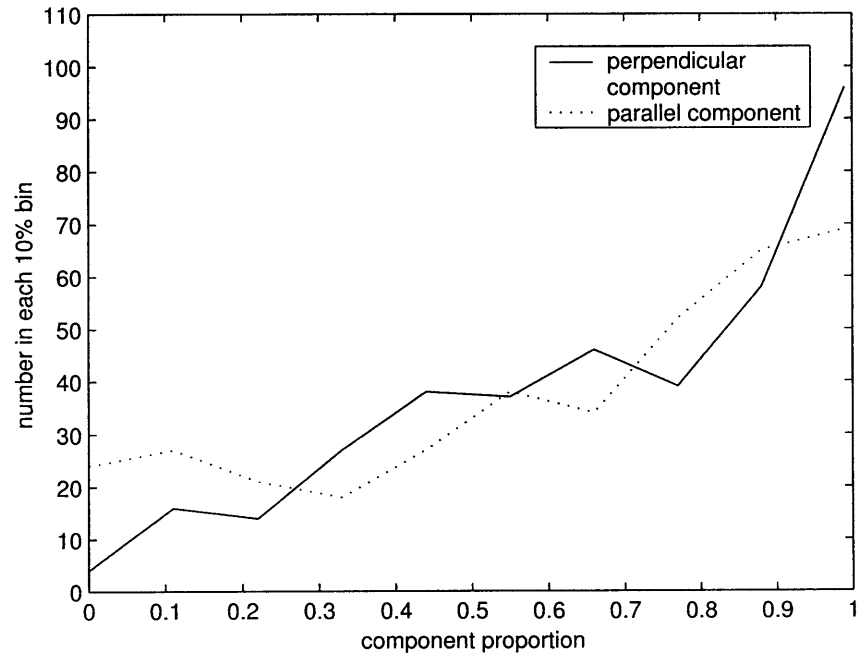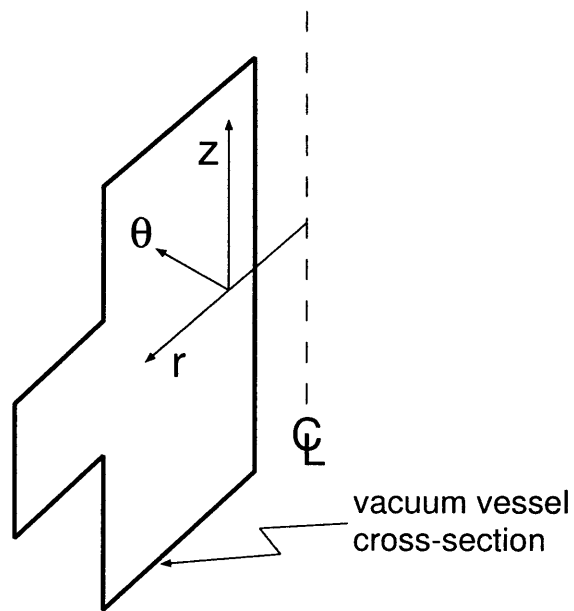Figure 4-8: Hodogram plot for $f_{fluc} > 2MHz$

34

Figure 4-9: VTF coordinates.

Chapter 5

Conclusions and Future Work

I have successfully designed and fabricated a three-axis magnetic fluctuation probe with a frequency response up to $100MHz$, to study turbulence in the VTF magnetic reconnection experiment. Even though the measurements in this thesis are preliminary, several important goals have been achieved, and several conclusions can be drawn. The FastB probe has been sucessful in measuring magnetic fluctuations from the ion gyro-frequency up into the lower-hybrid range. The high-frequency fluctuations seem to be preceded by low-frequency ones, and low frequency fluctuations travel largely in the toroidal direction.

The data collection was suddenly interrupted by a high-voltage power line failure. Once the power supply for the experiment is fixed, there is much work to do. Besides taking more fluctuation measurements once the new closed configuration is characterized, the plasma temperature, density, velocity, and potential need to be measured as well, to make better sense of the fluctuation measurements. These measurements can help pin down the structure and evolution of the current sheet. Also, the plasma resistivity must be measured to see whether or not it is being enhanced by fluctuation effects. This last task is necessary to establish a cause and effect relationship between fluctuations and reconnection rate.

The FastB probe will also be used to search for fluctuations in the open configuration. This will be a much less data collection-intensive job, since the open configuration has been extensively studied in the past. There is also work beyond the

37

FastB probe. Diagnostics need to be constructed to measure the wavelength of the fluctuations, with the goal of measuring their dispersion relation, and subsequently identifying the instability causing these fluctuations. This will require fabrication of a new multiple-fluctuation probe array, permitting cross-correlation measurements.

Bibliography

[1] D. Biskamp, *Magnetic Reconnection in Plasmas*, Cambridge University Press, Cambridge, England (2000)

[2] W. Daughton, Phys. Plasmas **10**, 3103 (2003)

[3] T. Carter, "Experimental Study of Fluctuations in a Reconnecting Current Sheet", Ph.D. Thesis, Princeton University (2001)

[4] J. Egedal *et al*, Rev. Sci. Instrum. **71**, 3351 (2000)

[5] H. Ji *et al*, Phys. Rev. Lett. **92**, 115001 (2004)